Final Results from the Jefferson Lab Q_{weak} Experiment and Constraints on Physics Beyond the Standard Model

G. Smith, on behalf of the Q_{weak} Collaboration*

Jefferson Lab, USA

E-mail: smithg@jlab.org

The Q_{weak} $\vec{e}p$ elastic scattering experiment used to extract an asymmetry at $Q^2 = 0.0248$ (GeV/c)^2 will be described. The final result was -226.5 ± 9.3 ppb- the most precise ep asymmetry ever measured. Some of the backgrounds and corrections applied in the experiment will be explained and quantified, and some of the experimental challenges will be described. Several methods used to extract consistent values of the proton's weak charge Q_W^p from our asymmetry measurement will be outlined. We also show the multi-TeV mass reach for beyond-the-Standard-Model physics obtained from our determination of the proton's weak charge, and discuss our sensitivity to specifc examples of new physics like compositeness. From the proton's weak charge, a result for the fundamental standard model parameter $\sin^2 \theta_W$ is obtained at the energy scale of our experiment. We compare that to the few other determinations of $\sin^2 \theta_W$ available in the literature, as well as the predicted behaviour based on SM input.

PACS: 12.15-y,14.20.Dh,14.65.Bt,25.30.Bf

---

*Speaker.

1. Introduction

A precise measurement of the proton's weak charge Q_W^p has long been viewed as a sensitive observable with which to test the standard model (SM). Q_W^p is highly suppressed due to the accidental cancellation of the individual weak charges of the quarks in the proton, which makes it a more sensitive probe of new physics on top of a small (suppressed) SM "background". At the same time, Q_W^p is accurately predicted [1] in the SM: $Q_W^{SM}(p) = 0.0708 \pm 0.0003$. We hope to find clues to physics beyond the SM (BSM) because despite its many successes, the SM has limitations. For example, it has too many parameters which are not predicted, and it fails to account for things like gravity, dark matter/energy, and the matter/antimatter asymmetry in the universe. Direct searches at colliders in the post-Higgs era have turned up little evidence of what the BSM physics might be. However, indirect searches utilizing precise measurements of well-predicted SM observables like Q_W^p have the potential to reach mass/energy scales beyond those directly accessible with high-energy accelerators.

On the other hand, the weak interaction is aptly named: it's a needle in the electromagnetic (EM) haystack. The ratio of the weak to the EM interaction is $\sim G_F Q^2/(4\pi\alpha\sqrt{2})$, where G_F and α are the Fermi and fine-structure constants, and Q^2 is the four-momentum transfer. At the Q^2 of the Q_{weak} experiment described below, this is only 2 ppm. How can it be isolated?

The solution is to exploit parity-violation (PV). The EM interaction conserves parity. The weak interaction does not. So we perform an elastic scattering experiment using a beam of longitudinally-polarized electrons and an unpolarized-proton target. We flip the spin of the electrons in the beam either parallel or anti-parallel to their momentum to mimic a parity reversal. The EM interaction doesn't change with this reversal. The weak interaction does. The observable we measure to isolate the weak interaction is the beam-spin asymmetry

$$A_{ep} = \frac{\sigma^+ - \sigma^-}{\sigma^+ + \sigma^-},$$

where $\sigma^\pm$ denotes the cross-section (probability) for detecting electrons with incoming helicity ± 1. At threshold ($\theta, Q^2 \to 0$), A_{ep} is proportional to $Q^2 Q_W^p$. Above threshold, hadronic structure contributions characterized with EM, strange quark, and axial form factors contribute as Q^4.

The Q_{weak} experiment [2] at Jefferson Lab in Newport News, VA was designed to perform a ppb-level $\vec{e}p$ asymmetry measurement at very low $Q^2 = 0.0248$ GeV^2 in order to measure A_{ep}, with which the proton's weak charge Q_W^p was determined for the first time [3, 4]. That led in turn to the determination of the most precise result for $\sin^2\theta_W$ below the Z-pole, and further enabled multi-TeV constraints to be placed on PV, semi-leptonic 4-point contact-interaction physics beyond the SM.

2. The Q_{weak} Experiment

The CEBAF accelerator at Jefferson Lab is a recirculating linac with a maximum energy near 12 GeV (6 GeV at the time of the Q_{weak} experiment). The need for low Q^2 led to the choice of an incident beam energy of 1.16 GeV and a lab scattering angle of 7.9°. The electron beam helicity was reversed on four time-scales: a fast 960 Hz pseudo-random reversal in $(\pm \mp \mp \pm)$ helicity

quartets using a Pockels cell in the polarized source, and three slow reversals using an insertable half-wave plate every 8 hours in the source, a monthly reversal in the injector using a double-Wien filter, and a single 2-month-long period at two-pass (instead of one-pass) which provided a g−2 reversal. The electron-beam polarization was measured continuously and non-invasively with a
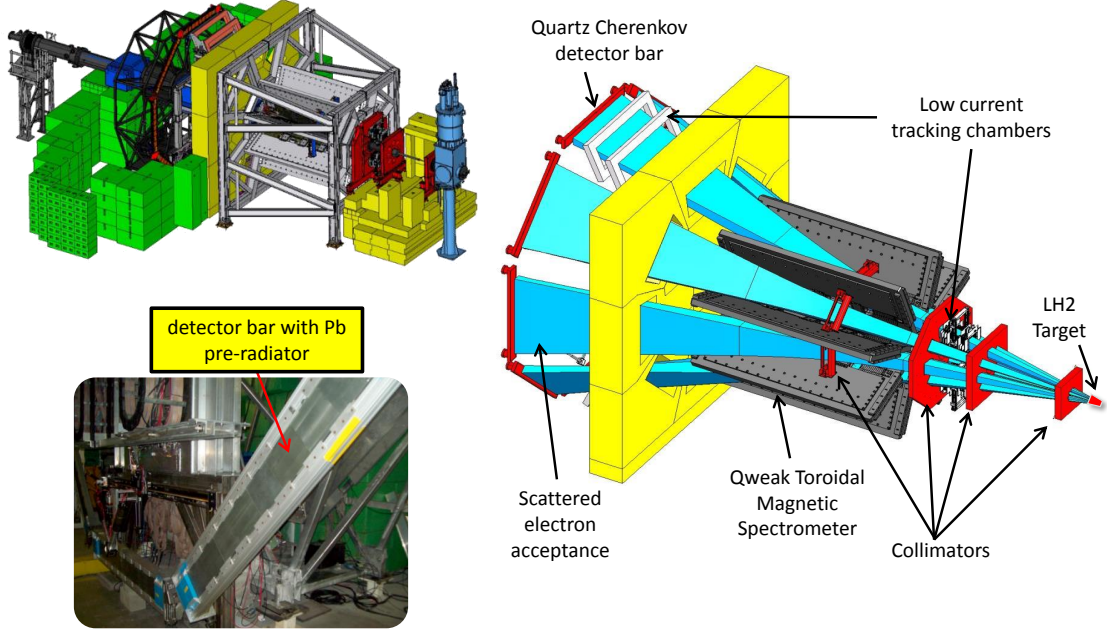

Figure 1: Views of the Q_{weak} experiment. Portions adapted from Reference [4].

Compton polarimeter built [5] for the experiment, and approximately twice per week in an invasive measurement using an existing [6] Møller polarimeter at only a few μA of beam current. These independent polarization-measurements were in good agreement with each other [7]. The average polarization was $88.7 \pm 0.61\%$.

The 58 l, 34.4 cm-long high-power LH2 target [8] built for this experiment was maintained at 20.00 K and 220 kPa. The beam was rastered (dithered) into a uniform 4x4 mm^2 spot on the 125 μm-thick aluminum entrance window. Consistent measures of the target density fluctuations near the helicity reversal frequency (aka target boiling) were measured several ways. At the 180 μA incident-beam current used in the experiment, the target noise was only 50 ppm over a 240 ms-long helicity quartet. The heating from the ionization energy-loss of the beam passing through the target was 2.2 kW- the total cooling power measured for the target was 3 kW.

Electrons scattered from the target passed through a series of three acceptance-defining colli-mators and then through a toroidal resistive-magnet onto eight 2-meter-long quartz Cerenkov de-tectors arrayed in a symmetric azimuthal pattern 3.44 m about the beam axis in a heavily-shielded

hut. Lead pre-radiators were placed just in front of these detectors to quench the soft-photon back-ground and raise the number of photoelectrons seen by the photomultiplier tubes (PMTs) on each end of each of the 8 detectors to about 100. These PMTs were operated in current (integrating) mode since each detector experienced rates of about 900 MHz. The main features of the experi-ment are described in detail in [2, 3, 4] and depicted in Figure 1.

A raw asymmetry A_{raw} was determined in the Q_{weak} experiment from the difference over the sum of beam-charge-normalized detector yields $Y^{\pm}$ determined for each ± 1 helicity state of the beam. This raw asymmetry was then corrected for various (measured) false asymmetries to form A_{msr}:

$$A_{\text{msr}} = A_{\text{raw}} + A_T + A_{NL} + A_{\text{BCM}} + A_{\text{BB}} + A_{\text{beam}} + A_{\text{bias}}, \tag{2.1}$$

where A_T accounted for the residual contribution from transversely-polarized electrons in the beam, A_{NL} for the detector non-linearity, A_{BCM} for the observed variation in beam-current-monitor results, A_{BB} for contributions from beam-halo interactions in the beamline and beam collimator just down-stream of the target, A_{beam} for the helicity-correlated false asymmetries in the beam associated with position, angle, and energy, and A_{bias} for a rescattering of electrons which picked up a transverse-polarization via g-2 precession in the spectrometer field, which led to an asymmetry in the lead pre-radiators fronting the main detectors. Backgrounds were subtracted which arose from the thin aluminum target windows (b_1), inelastics (b_4), and a residual soft-photon background from sec-ondary scattering in the beamline (b_3). These backgrounds were determined by measuring their asymmetries A_i and signal dilutions f_i. A multiplicative correction-factor $R_{tot} = 0.973 \pm 0.008$ was formed by considering 4 factors: EM radiative corrections, the detector response to Q^2/position, a finite-acceptance Q^2 correction $A(<Q^2>)/<A(Q^2)>$, and a correction which folded the Q^2 uncertainty into the asymmetry. All of this comes together according to

$$A_{ep} = R_{\text{tot}} \frac{A_{\text{msr}}/P - \sum_{i=1,3,4} f_i A_i}{1 - \sum_{i=1}^{4} f_i}, \tag{2.2}$$

where P denotes the longitudinal beam polarization. The contributions of each of these components is shown in Figure 2a. The stability of the asymmetry over time with respect to the three slow spin-reversals is shown in Figure 2b.

3. Extracting Q_W^p

With the asymmetry from the Q_{weak} experiment in hand, we could determine Q_W^p from that datum by itself, or in conjunction with other asymmetry measurements of $\vec{e}p$, $\vec{e}d$, and $\vec{e}\,^4He$ elas-tic scattering. In either case the starting point is the tree-level formula connecting the measured asymmetry on the proton A_{ep} with the electromagnetic (EM) form factors $G_{E,M}^{\gamma}$, the proton's weak neutral form factor $G_{E,M}^{pZ}$, and the axial form factor G_A^Z:

$$A_{ep} = \left[\frac{-G_F Q^2}{4\pi\alpha\sqrt{2}} \right] \left[\frac{\varepsilon G_E^{\gamma} G_E^Z + \tau G_M^{\gamma} G_M^Z - (1 - 4\sin^2\theta_W)\varepsilon' G_M^{\gamma} G_A^Z}{\varepsilon (G_E^{\gamma})^2 + \tau (G_M^{\gamma})^2} \right], \tag{3.1}$$

where

$$\varepsilon = \frac{1}{1 + 2(1+\tau)\tan^2\frac{\theta}{2}}, \quad \varepsilon' = \sqrt{\tau(1+\tau)(1-\varepsilon^2)} \tag{3.2}$$

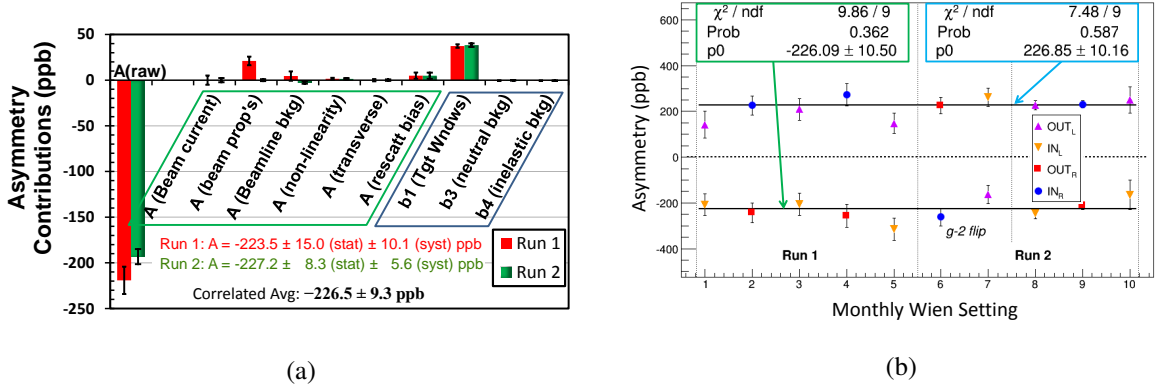Figure 2: (a) Uncertainty contributions to the asymmetry. (b) Observed PV asymmetry A_{ep} in the Q_{weak} experiment after all corrections, versus the double-Wien-filter beam-helicity configuration (L/R), reversed monthly (see [4]). The insertable half-wave plate at the electron source generated an additional $180°$ flip of the spin when IN. A period in which a further $180°$ flip was generated through $(g_e - 2)$ precession is also indicated. Solid lines represent the time-averaged values. The uncertainties $(1\,\sigma)$ shown are those of the corresponding A_{msr} values (see text) only- they do not include time-independent uncertainties in order to illustrate the time stability of the results. Adapted from Reference [4].

are kinematical quantities, Q^2 is the four-momentum transfer, $\tau = Q^2/4M^2$ where M is the proton mass, G_F is the Fermi coupling constant, α is the fine structure constant and θ is the laboratory electron scattering-angle. The weak neutral form factor $G_{E,M}^{pZ}$ can be written in terms of the proton's EM form factors and the strange-quark form factors $G_{E,M}^s$ using isospin symmetry:

$$G_{E,M}^{pZ} = \left(1 - 4\sin^2\theta_W\right) G_{E,M}^{p\gamma} - G_{E,M}^{n\gamma} - G_{E,M}^{s\gamma} = Q_W^p G_{E,M}^{p\gamma} - G_{E,M}^{n\gamma} - G_{E,M}^{s\gamma}. \tag{3.3}$$

Substituting equation 3.3 into equation 3.1, the asymmetry can be reduced to a simpler expression when $\theta \to 0$, $\varepsilon \to 1$, and $\tau << 1$:

$$A_{ep} = A_0 \left[Q_W^p + Q^2 B(Q^2, \theta)\right], \text{ where } A_0 = \left[\frac{-G_F Q^2}{4\pi\alpha\sqrt{2}}\right]. \tag{3.4}$$

It's clear from equation 3.4 that in a plot of A_{ep}/A_0, Q_W^p is the intercept, and the hadronic structure represented by all the form factors is encapsulated in the $Q^2 B(Q^2, \theta)$ "slope" term. The Q_{weak} collaboration chose to include all the existing 28 $\vec{e}p$ asymmetries [9, 10, 11, 12, 13, 14, 15, 16, 17, 18] up to a Q^2 of 0.63 GeV^2, including Q_{weak} 's results [3, 4], along with 5 $\vec{e}d$ [10, 18, 20, 21] and 2 $\vec{e}\,^4He$ asymmetries [13, 19] in a global fit. The fit varied the weak vector quark couplings C_{1u} and C_{1d}, the axial form factors G_A^p and G_A^n, and the overall magnitudes ρ_s and μ_s of the strange electric and magnetic form factors G_E^s and G_M^s. The small isoscalar combination of the axial form factors $G_A^{Z(T=0)} = (G_A^p + G_A^n)/2$ was constrained by the calculation of [22], leaving five effective parameters in the fit. A dipole form $G_D = (1 - Q^2/\lambda^2)^{-2}$ with $\lambda = 1$ GeV was used to describe the Q^2 dependence of G_A. The strange form factors were taken to be $G_E^s = \rho_s Q^2 G_D$ and $G_M^s = \mu_s G_D$

4

following the work of [23]. The intercept of the fit shown in figure 3a is $Q_W^{g.f}(p) = 0.0719 \pm 0.0045$, where the superscript "gf" refers to the global fit used for this result, described above. It agrees well (0.2σ) with the SM prediction $Q_W^{SM}(p) = 0.0708 \pm 0.0003$ found in [1].

A number of other methods were explored to extract the weak charge from the Q_{weak} asymmetry, with and without the PVES database. First, the result of the global fit was combined with the precise atomic PV (APV) result on ^{133}Cs [24, 25, 26]- no improvement in Q_W^p was observed,

(a)   (b)

Figure 3: (a) Global fit (see [4]) (black curve) of the reduced asymmetries A/A_0 constituting the PVES database. The yellow band indicates the uncertainty in the fit. The inset shows the region of the Q_{weak} experiment which dominates the fit. The legend indicates the different collaborations responsible for the data used in the fit, and also indicates the SM value of Q_W^p with the black arrowhead at $Q^2 = 0$. Adapted from Reference [4]. (b) Different determinations of Q_W^p using the Q_{weak} datum with and without the other PVES asymmetries, fitting some of the form factors to the PVES data or calculating them as described in the text.

although the uncertainties on the individual vector weak charges improved. Another result was obtained by constraining $G_{E,M}^s$ to the lattice quantum chromodynamics (LQCD) calculations of [27], and then refitting the PVES data with the Q_{weak} datum using 3 effective parameters instead of 5. An interesting extraction was made using just the Q_{weak} datum, without any of the other PVES data, and calculating the hadronic structure form factors $G_{E,M}^{p,n}$ [28], $G_{E,M}^s$ [27], and G_A [29]. The latter two form factors are relatively small at the kinematics of the Q_{weak} experiment. Interestingly, the uncertainty from this result using the Q_{weak} datum alone is similar to that obtained with the global fit method which employed the entire PVES database. Finally, this last method employing calculated form factors was extended to the entire PVES database, extracting a "Q_W^p" from each datum, and fitting those with a straight line. The intercept of that line was almost identical to that obtained with the global fit using the LQCD constraint. The results from all these different approaches are summarized graphically in figure 3b.

4. Mass Reach for BSM Physics

The Q_W^p result can be used to set mass limits for potential new semi-leptonic, PV arbitrary

four-point contact interaction BSM physics by considering the Lagrangian:

$$\mathcal{L}_{PV}^{msrd} = \mathcal{L}_{NC}^{SM} + \mathcal{L}_{PV}^{new} \tag{4.1}$$

$$= \bar{e}\gamma_\mu\gamma_5 e \sum_q \left(\frac{G_F}{\sqrt{2}}C_{1q} + \frac{g^2}{\Lambda^2}h_V^q\right)\bar{q}\gamma^\mu q. \tag{4.2}$$

$$\tag{4.3}$$

Here h_V^q represents the projections of the u,d flavor mixing angle $\theta_h = \tan^{-1}(N_d/N_u)$: $h_V^u = \cos\theta_h$ and $h_V^d = \sin\theta_h$. Equation 4.2 can be easily rearranged into the polar form of a circle in C_{1q} space:

$$\left(C_{1u}^{msrd}, C_{1d}^{msrd}\right) = \left(C_{1u}^{SM}, C_{1d}^{SM}\right) + r\left(\cos\theta_h + \sin\theta_h\right), \tag{4.4}$$

with radius

$$r = \frac{\sqrt{2}}{G_F}\left(\frac{g}{\Lambda}\right)^2. \tag{4.5}$$

These circles are plotted (see [4]) in figure 4. Also shown in that figure are the constraints provided
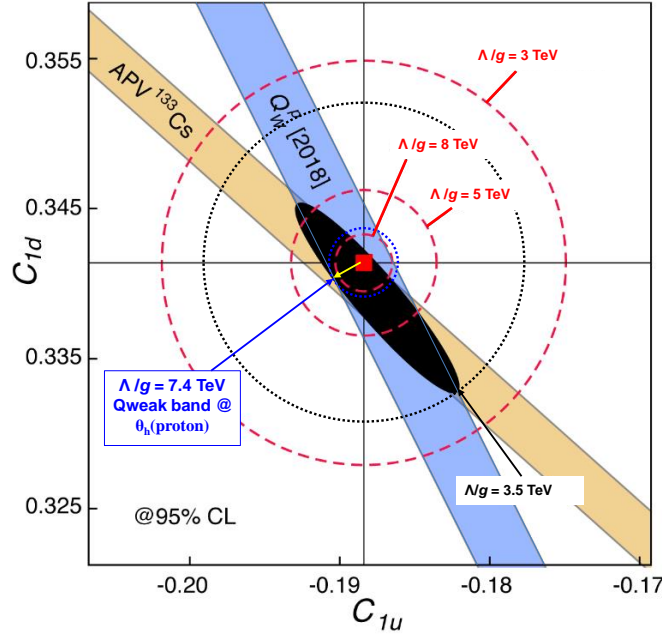

Figure 4: Contours of mass reach in weak vector coupling C_{1q} space (dashed circles), along with the constraints provided by the Q_{weak} experiment (blue band), the cesium APV experiment (orange band), or both together (black ellipse). Adapted from Reference [4].

by the Q_W^p experiment's result [4] $Q_W(p) \pm \Delta Q_W(p) = -2(2C_{1u}+C_{1d}) = 0.0719 \pm 0.0045$, and that of the cesium APV experiment [24, 25, 26] $Q_W(^{133}Cs) = -2(188C_{1u}+211C_{1d}) = -72.62 \pm 0.43$, as well as both combined. The mass reach provided by the Q_{weak} experiment by itself is identified as the distance between the SM origin and the lines defined by the Q_{weak} band. The larger of these 2 distances corresponds to the smaller mass reach, and thus the mass below which the Q_{weak} experiment rules out semi-leptonic PV 4-point contact interaction BSM physics: $\Lambda/g = 7.5$ TeV. With the coupling $g^2 = 4\pi$ associated with compositeness which is typically used to compare the mass reach of different experiments, this corresponds to $\Lambda = 26.6$ TeV.

5. The Weak Mixing Angle

The weak mixing angle is a fundamental parameter of the SM which describes the mixing of the EM and weak interactions. At tree level, its value is defined by the masses of the charged $W^{\pm}$ and neutral Z^0 bosons: $1 - \sin^2 \theta_W = (M_W/M_Z)^2$. Despite its importance in the electroweak theory of the SM, its value is not predicted- it must be measured. However, electroweak theory does predict that it depends on scale (momentum transfer Q) so this predicted "running" of $\sin^2 \theta_W$ can also be tested. Q_W^p and $\sin^2 \theta_W$ are related via various electroweak radiative corrections: box diagrams ($\Box_{WW}$, $\Box_{ZZ}$, $\Box_{\gamma Z}$), vertex corrections (Δ_e, Δ'_e), and a strength renormalization (ρ_{NC}) as follows:

$$4 \sin^2 \theta_W(0) = 1 - \frac{Q_W^p - \Box_{WW} - \Box_{ZZ} - \Box_{\gamma Z}(0)}{\rho_{NC} + \Delta_e} + \Delta'_e \tag{5.1}$$

Details are provided in [4]. The result from the Q_{weak} experiment is shown (see [4]) in fig-
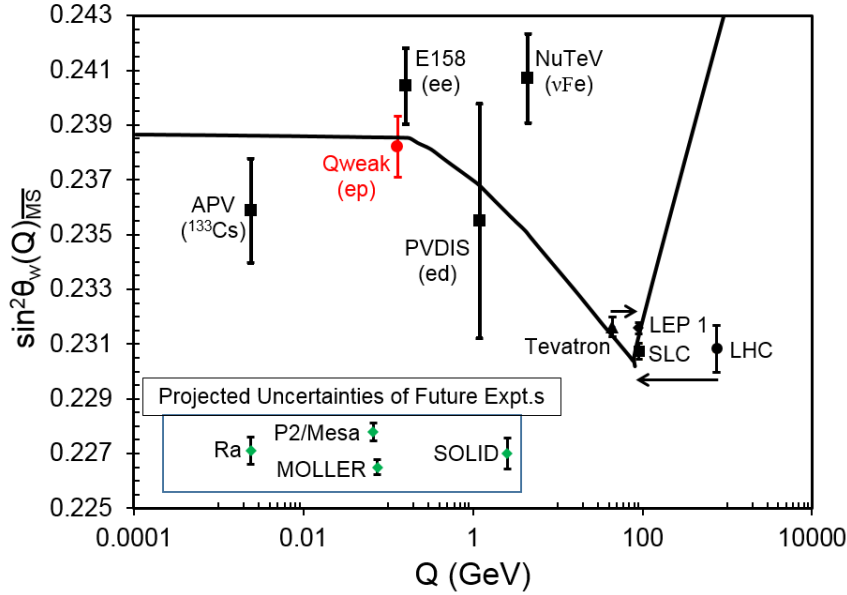

Figure 5: Various experimental determinations of $\sin^2 \theta_W$. The most precise determination below the Z^0-pole is provided by the Q_{weak} experiment (red datum). The goals of future efforts to measure Q_W^e [30], and Q_W^p [31] in particular, are shown in green. Adapted from Reference [4].

ure 5 along with determinations near the Z^0-pole [1], as well as other low Q determinations from APV [24, 25, 26], Møller scattering [32], and a neutrino-nucleus result [33] which did not include important nuclear corrections [34] which have the effect of putting that νN result smack on the running curve of [1].

Acknowledgments

References

[1] Patrignani C, et al. (Particle Data Group), *Chin. Phys. C* **40** 100001 (2016)

[2] T. Allison, et al., (Q_{weak} Collaboration), *Nucl. Instrum. Meth. A* **781** 105 (2015)

[3] D. Androić et al., (Q_{weak} Collaboration), *Phys. Rev. Lett.* **111** 141803 (2013)

[4] D. Androić et al., (Q_{weak} Collaboration), *Nature* **557** 207 (2018)

[5] Narayan, et al., *PRX* **6** 011013 (2016)

[6] M. Hauger et.al., *Nucl Inst.& Meth. A* **462** 382 (2001)

[7] Magee, J. et al., *Phys. Lett. B* **76** 339 (2017)

[8] G.R. Smith, *Nuovo Cimento Soc. Ital. Fis. C*, **35** 159 (2012)

[9] D.S. Armstrong, et al. (G0 Collaboration), *Phys. Rev. Lett.* **95** 092001 (2005)

[10] D. Androić et al., (G0 Collaboration), *Phys. Rev. Lett.* **104** 012001 (2010)

[11] K.A. Aniol, et al., (HAPPEX Collaboration), *Phys. Rev. C* **69** 065501 (2004)

[12] K. A. Aniol, et al., (HAPPEX Collaboration), *Phys. Lett. B* **635** 275 (2006)

[13] A. Acha, et al., (HAPPEX Collaboration), *Phys. Rev. Lett.* **98** 032301 (2007)

[14] Z. Ahmed, et al., (HAPPEX Collaboration), *Phys. Rev. Lett.* **108** 102001 (2012)

[15] D.T. Spayde, et al., *Phys. Lett. B* **583** 79 (2004)

[16] F.E. Maas, et al., *Phys. Rev. Lett.* **93** 022002 (2004)

[17] F.E. Maas, et al., *Phys. Rev. Lett.* **94** 152001 (2005)

[18] S. Baunack, et al., *Phys. Rev. Lett.* **102** 151803 (2009)

[19] K. A. Aniol, et al., (HAPPEX Collaboration), *Phys. Rev. Lett.* **96** 022003 (2006)

[20] D. Balaguer Ríos, et al., *Phys. Rev. D* **94** 051101 (2016)

[21] T. M. Ito, et al., (SAMPLE Collaboration), *Phys. Rev. Lett.* **92** 102003 (2004)

[22] S.L. Zhu, S.J. Puglia, B.R. Holstein, M.J. Ramsey-Musolf, *Phys. Rev. D* **62** 033008 (2000)

[23] R.D. Young, J. Roche, R.D. Carlini, A.W. Thomas, *Phys. Rev. Lett.* **97** 102002 (2006)

[24] S.C. Bennett, C.E. Wieman, *Phys. Rev. Lett.* **82** 2484 (1999)

[25] C.S. Wood, et al., *Science* **275** 1759 (1997)

[26] J.S.M. Ginges, V.V. Flaumbaum, *Phys. Rep.* **397** 63 (2004)

[27] J. Green, et al., *Phys. Rev. D* **92** 031501 (2015)

[28] J. Arrington, I. Sick, *Phys. Rev. C* **76** 035201 (2007)

[29] J. Liu, R.D. McKeown, M.J. Ramsey-Musolf, *Phys. Rev. C* **76** 025202 (2007)

[30] J. Benesch, et al., [nucl-ex/1411.4088].

[31] D. Becker et al., [nucl-ex/1802.04759]

[32] P.L. Anthony et al., *Phys. Rev. Lett.* **95** 08161 (2005)

[33] G. P. Zeller et al., (NuTeV), *Phys. Rev. Lett.* **88** 091802 (2002)

[34] W Bentz, I.C. Cloët, J.T. Londergan, A.W. Thomas, *Phys. Lett. B* **693** 462 (2010)

PoS(SPIN2018)008